NASA Technical Memorandum 86293

NASA-TM-86293 19840024435

RESPONSE OF INCONEL 617 SUPERALLOY TO COMBINED GROUND-BASED AND STS REENTRY EXPOSURE

RONALD K. CLARK
JALAIAH UNNAM

AUGUST 1984

NASA
National Aeronautics and
Space Administration

Langley Research Center
Hampton, Virginia 23665

RESPONSE OF INCONEL 617 SUPERALLOY TO COMBINED GROUND-BASED AND STS REENTRY EXPOSURE

RONALD K. CLARK*
NASA-LANGLEY RESEARCH CENTER
HAMPTON, VA 23666

AND

JALAIAH UNNAM**
ANALYTICAL SERVICES AND MATERIALS, INC.
TABB, VA 23602

Abstract

Inconel 617 is a nickel-based superalloy which is being considered for heat-shield applications because of its high-temperature strength, good oxidation resistance and high emittance of oxidized surfaces. While the effects of simulated reentry conditions on emittance and oxidation of Inconel 617 have been studied, the combined effects of the ground-based environment with sea salt exposure and the reentry environment have not been evaluated. Experimental results are presented to show the effects of environmental simulation including ground-based and reentry exposure on the emittance and oxidation of Inconel 617. Specimens were exposed to simulated reentry at a surface temperature of 2000°F in the Langley Research Center Hypersonic Materials Environmental Test System (HYMETS) Facility with and without alternate exposures to an atmospheric seashore environment or a laboratory sea salt environment. This paper presents emittance, mass loss, oxide chemistry, and alloy composition data for the specimens.

Introduction

The metallic heat shield concept continues to be of strong interest for the radiatively cooled thermal protection system (TPS) for advanced reuseable space transportation vehicles[1] and hypersonic aircraft[2]. Nickel-chromium superalloys in general have been shown to possess the desirable characteristics of high-temperature strength and excellent long-term oxidation resistance which are prerequisites to successful performance of metallic TPS.[3-8] In addition, efficient radiative TPS must have a high, stable emittance for up to 100 flights. Inconel 617 has been shown to meet the high-temperature strength/oxidation resistance criteria and its surface has a relatively high emittance (about 0.8) for up to 100 exposure cycles.[9-11] However, the response of Inconel 617 to the more realistic environment that couples ground-based exposure, including the presence of sea salt, with space transportation system (STS) reentry exposure has not been examined. Concerns for the effects of sea salt exposure on performance of Inconel 617 are heightened by reports that hot corrosion of some superalloys is a problem in engine applications.[12]

The purpose of this research was to define the effects of combined ground-based and STS reentry exposure on the emittance and oxidation characteristics of Inconel 617. Specimens were exposed to simulated reentry at a surface temperature of 2000°F in the Langley Research Center HYMETS Facility with and without alternate exposures to a seashore environment or a laboratory sea salt environment.

Experimental Procedures

Test Specimens

Test specimens were stamped from an 0.030-inch thick sheet of Inconel 617. The specimens were disks 1.0 inch in diameter with three, 3/16 x 3/16 inch, radial projections spaced 120 degrees on centers for mounting the specimens during reentry exposure. Table 1 gives the chemical analysis of the material as provided by the certification of test report from the vendor.

Table 1. Inconel 617 Analysis

Element	Weight Percent
Ni	53.20
Cr	22.63
Co	12.33
Mo	9.38
Al	1.15
Fe	.76
Ti	.27
Si	.15
C	.06
Cu	.05
Mn	.02
S	.001

Exposure of Specimens

Specimens were statically oxidized for 12 hours at 1800°F in laboratory air to give a high emittance before the start of reentry testing. Prior to static oxidation specimens were

* Research Scientist
** Senior Scientist

thoroughly cleaned to assure that they were free of oils.

Specimens were exposed to cyclic conditions of simulated STS reentry with and without alternate exposures to a seashore environment or a laboratory sea salt environment. The simulated reentry tests were half-hour exposures at a surface temperature of 2000°F in the Langley Research Center HYMETS Facility. The seashore environmental tests were two-week exposures on a specimen rack located at the east end of the Langley Air Force Base runway about one hundred feet from a salt water inlet from the Chesapeake Bay. The laboratory sea salt tests were 24- to 72-hour exposures where the specimens were dipped in sea water then hung over the sea water bath in a closed container.

The HYMETS Facility is an Acurex Corporation 100-kw constrictor-arc-heated wind tunnel.[13] Fig. 1 shows a schematic of the test setup. It consists of a segmented constrictor-arc heater, a test chamber with three model insertion stings and continuous duty vacuum pumps. Specimens are mounted on stagnation model adaptors attached to the insertion stings. Another sting contains a water-cooled heating rate/pressure probe which was used to measure the cold wall heating rate and the surface pressure. The test gas is a mixture of air plus nitrogen and oxygen in ratios equivalent to air. High purity nitrogen is introduced at the down stream end of the cathode. Air and high purity oxygen are introduced in the plenum and mixing chamber. The nominal operating conditions for simulated reentry testing of the specimens are given in Table 2.

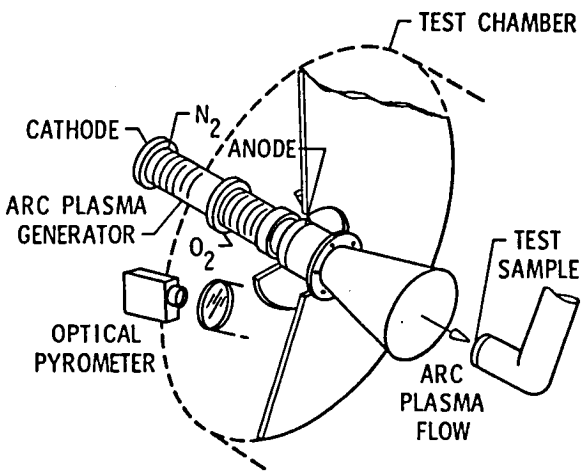

Fig. 1 Schematic of Langley Research Center HYMETS facility for simulated reentry testing.

Analyses of Oxidation

Mass changes of specimens were determined by weighing specimens after the initial static oxidation and after each reentry cycle. The mass change data were used to estimate substrate thickness changes and as a basis of comparison for specimens with different exposure conditions.

Table 2. HYMETS operating conditions for simulated STS reentry exposure of specimens

Specimen Surface Temperature, °F	2000
Surface Pressure, Torr	4.7
Free Stream Mach Number	3.3
Free Stream Enthalpy, Btu/lb	2400
Cold Wall Heating Rate, Btu/ft^{2}sec	18-20

The morphology of specimen oxides was studied using conventional light microscopy and scanning electron microscopy (SEM) at magnifications up to 1500X. The oxide composition was analyzed by energy dispersive X-ray analysis (EDAX), by X-ray diffraction analysis (XRD), and by electron microprobe (EMP).

Microprobe analyses of polished cross-sections of oxidized specimens were performed to determine the substrate elemental composition profiles. Compositional analyses were conducted at known locations beginning at the oxide-substrate interface and progressing to the interior. The microprobe was also used to determine the oxide thickness by making line scans across the polished cross-sections.

Radiative Property Measurement

Room temperature near-normal reflectance measurements were made on pre- and post-exposure specimens using a Gier-Dunkle DB100 reflectometer and a Gier-Dunkle Model HCDR-3 heated cavity reflectometer. The DB 100 reflectometer measures the total room temperature reflectance. The heated cavity reflectometer was used to make spectral reflectance measurements over the wavelength range from 2 to 25 μm. The reflectance data were used with Kirchoff's Law to arrive at corresponding values of emittance. The spectral data were integrated with respect to the Planck blackbody energy distribution curve for 2000°F to arrive at the total normal emittance at 2000°F.

A limited number of near-normal spectral emittance measurements were made at 2000°F for comparison with the emittance data derived from reflectance measurements. The spectral emittance measurements were made over the wavelength range from 1 to 15 μm using a radiometric technique.[14]

Results and Discussion

Table 3 presents a summary of the mass loss and emittance results for combined ground-based and reentry exposure of Inconel 617. Data are shown for specimens in the statically oxidized condition, after exposure to simulated reentry, after exposure to combinations of reentry and atmospheric or laboratory sea salt conditions, and after exposure to simulated reentry with oxide removal.

Oxidation Characteristics

The mass loss data in Table 3 are shown graphically in Fig. 2. Each data point represents a loss in mass with exposure compared to short-time static oxidation data for Inconel 617 which shows a mass increase of about 0.1 mg/cm^2 after five hours of static oxidation at 2000°F.[15]

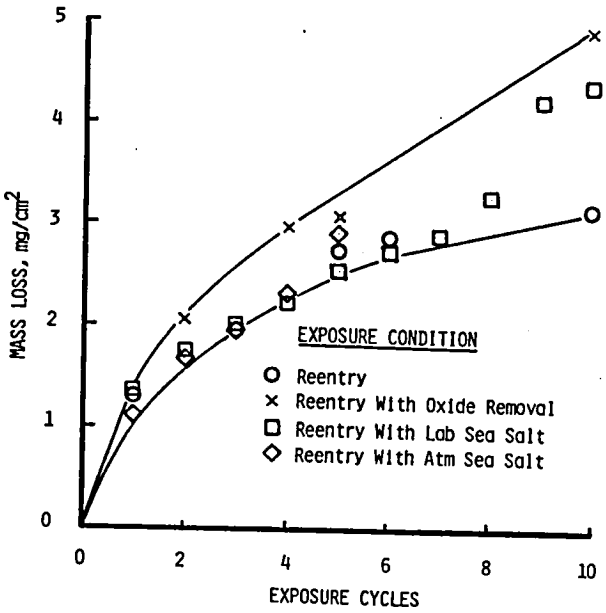

Fig. 2 Mass loss of Inconel 617 with TPS exposure.

The data for the exposure condition designated "Reentry with Oxide Removal" represents the "worst case" for mass loss since the oxide was removed with a stiff bristle brush after each simulated reentry cycle. The "mildest case" is the exposure consisting of simulated reentry with no sea salt exposure. The difference in mass loss for these extremes increases with number of exposure cycles. Beyond four exposure cycles specimens subjected to atmospheric and laboratory sea salt conditions experience a slightly greater mass loss than do specimens subjected to simulated reentry with no sea salt exposure. Mass changes of the order presented here represent substrate thickness decreases of the order of 2-10 μm.

Fig. 3 shows SEM photographs of the surface oxides of specimens for different exposure conditions. The statically formed oxide (Fig. 3(a)) is flat and uniform much like the faceted structure of unoxidized Inconel 617. SEM photographs of specimens after simulated reentry with and without sea salt exposure (Figs. 3(b) and 3(c)) show spherical oxide particles at the surface which are typical of the oxide morphologies reported in the literature for dynamically oxidized superalloys.[5,7,8,16] Evidence of disruption of the oxide by sea salt

Table 3. Summary of results for combined ground-based and reentry exposure of Inconel 617.

Spec. No.	Exp. Cond.*	No. Cycles	Heating Rate, Btu/ft²s	Surface Press., Torr	Stream Enthalpy, Btu/lb	Mass Loss, mg/cm²	Total Emittance			
							Room Temp		2000°F	
							HCRA	DB 100	HCRA	HTEA
I-227	AR	--	--	--	--	--	0.68	0.68	0.86	0.82
I-208	R	1	18.6	4.7	2425	1.24	0.77	0.76	0.90	---
I-209	R	1	17.0	4.8	2205	1.40	0.78	0.77	0.90	---
I-219	R	3	17.9	4.8	2315	2.04	0.81	0.80	0.89	---
I-221	R	3	19.0	4.8	2455	1.96	0.82	0.80	0.89	---
I-229	R	6	--	--	--	2.62	0.84	--	0.87	---
I-231	R	6	--	--	--	2.88	0.86	0.83	0.87	---
I-11	R	10	--	--	--	--	0.85	0.83	0.87	---
I-15	R	10	--	--	--	--	0.90	0.88	0.79	---
I-211	R	10	--	--	--	3.45	0.87	0.85	0.89	---
I-220	R	10	--	--	--	3.40	0.86	--	0.80	---
I-223	R	10	17.8	4.7	2325	2.89	0.86	0.83	0.87	0.83
I-224	R	10	18.3	4.7	2385	2.91	0.84	---	0.88	---
I-19	R	31	--	--	--	--	0.91	0.89	0.80	---
I-20	R	31	--	--	--	--	0.92	0.89	0.80	---
I-202	RL	2	17.0	4.8	2205	1.57	0.81	0.79	0.88	---
I-205	RL	3	18.0	4.6	2375	2.03	0.84	0.82	0.87	---
I-216	RL	6	--	--	--	3.08	0.81	--	0.81	---
I-213	RL	10	--	--	--	4.39	0.80	--	0.81	---
I-206	RA	2	19.8	4.8	2545	1.72	0.80	0.79	0.89	---
I-204	RA	5	17.1	4.5	2285	2.78	0.82	--	0.88	---
I-214	RA	5	20.0	4.8	2575	3.04	0.84	--	0.86	---
I-210	RO	5	16.8	4.4	2275	3.07	0.84	0.82	0.88	---
I-212	RO	10	20.8	4.4	2885	4.91	0.86	--	0.87	---
I-203	ROX	10	17.3	4.6	2285	--	0.73	0.73	0.82	---

*Exposure Conditions:

AR - statically oxidized for 12 hours at 1800°F, furnace cooled
R - simulated reentry at 2000°F surface temperature
RL - simulated reentry with laboratory exposure to sea salt
RA - simulated reentry with atmospheric exposure to sea salt
RO - simulated reentry with mechanical removal of oxide between cycles
ROX - simulated reentry with mechanical removal of oxide after 10 cycles

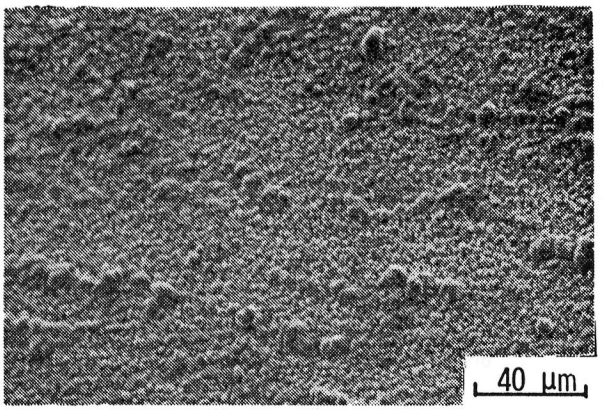

(a) Statically oxidized.

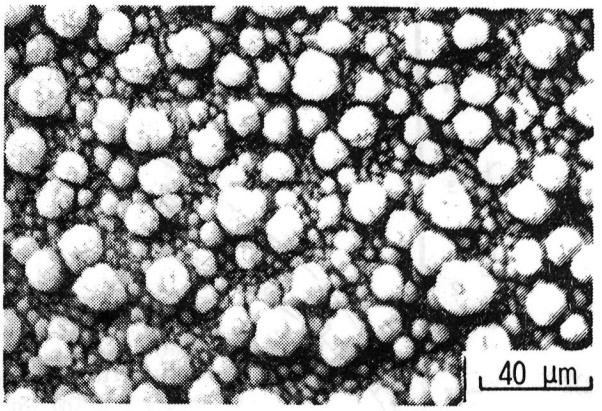

(b) Simulated reentry, 10 cycles.

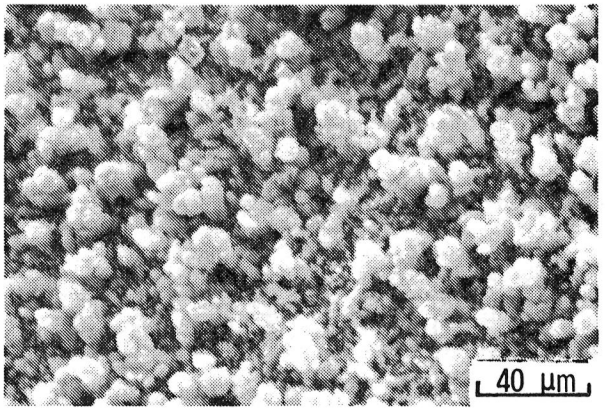

(c) Simulated reentry with lab sea salt, 10 cycles.

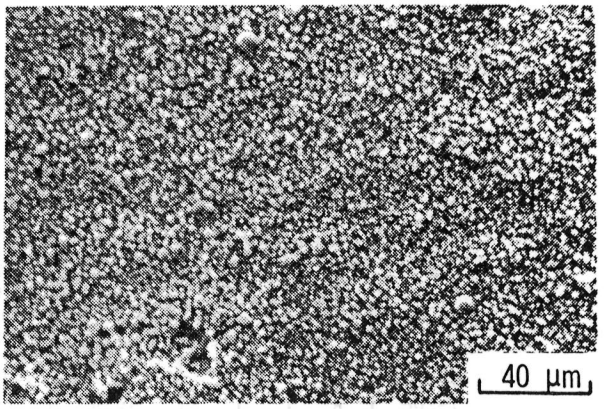

(d) Simulated reentry with atm sea salt, 5 cycles.

Fig. 3 SEM photographs of Inconel 617 oxide surfaces.

exposure is present in Fig. 3(c) which shows some irregularities in the spherical oxide particles and in Fig. 3(d) which shows no spherical particles.

The fragile nature of oxides of Ni-Cr alloy oxidized under dynamic conditions has been a cause for concern. The SEM photograph of the specimen after reentry with atmospheric exposure shows that the oxide is weathered to the extent that the spherical oxide particles have been removed; however, the mass data in Fig. 2 show the sea salt exposure specimens experienced only slightly greater mass loss than specimens exposed to reentry alone.

Table 4 presents data from analysis of specimens using EDAX, XRD, and EMP. These data indicate that the statically formed oxide of Inconel 617 is Cr_2O_3. Specimens exposed to simulated reentry have a high NiO-content and a minor $CoCr_2O_4$-content in the surface oxide. The NiO exists primarily as spherical oxide particles on top of a Cr_2O_3-rich suboxide and the $CoCr_2O_4$ exists as a minor constituent in the suboxide.

The oxide chemistry data for specimens after sea salt exposure are not notably different from the data for specimens with no sea salt exposure. The absence of any evidence of chemical species characteristic of sea salt indicates that salt deposits from sea salt exposure are quickly volatilized on exposure to reentry conditions and do not react with the surface oxide.

The microprobe line scan data in Table 4 show the oxide thickness and alloy depletion depth for a number of specimens. The oxide thickness ranges from 5 μm for the statically formed oxide to 6-7 μm for specimens after exposure to 10 reentry cycles.

Chromium and aluminum are selectively oxidized on exposure to reentry conditions resulting in an alloy depletion zone near the surface where

the composition varies from the base alloy chemistry.

Figure 4 shows quantitative compositional analysis data for the metal substrate of a typical specimen. The zone that was affected by diffusion of metal atoms to the surface is about 35 μm thick. Cr has been reduced to one-fourth the base alloy level at the oxide-substrate interface. Aluminum is similarly reduced. Ni, Co, and Mo experience an increase in weight fraction at the interface due to the loss of Cr. XRD analysis of the surface oxide did not indicate the presence of aluminum containing compounds; however, it is likely that the small amount of Al lost from the substrate exists as a thin subscale of Al_2O_3 and/or substitutional atoms in other oxides.

The data in Table 4 show the depleted zone to range from 19 μm in depth for the statically oxidized specimen to 47 μm in depth for the most severe case of reentry with oxide removal after each cycle. The alloy-depleted zone of specimens exposed to reentry with and without sea salt exposure was 30-35 μm in depth. Alloy depletion zone thicknesses of the order seen here comprise only about five percent of the total thickness of the specimens in this program, hence there remains a major portion of undisturbed alloy and there should be ample mechanical performance to meet the needs in TPS applications. In applications using very thin sheet (0.006-0.010 inch), the effect of alloy depletion on mechanical properties should be investigated.

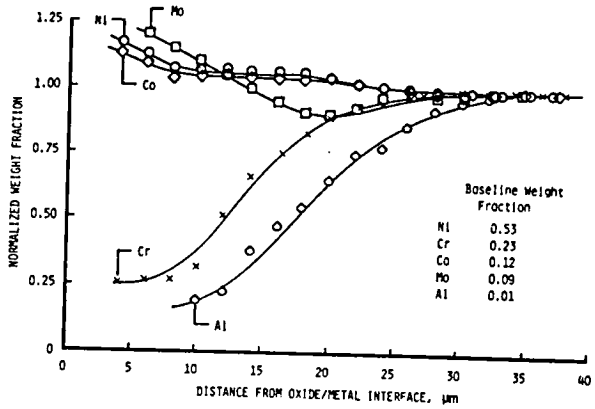

Fig. 4 Elemental composition profiles of Inconel 617 metal substrate.

Radiative Properties

Room temperature reflectance data obtained with the heated cavity reflectance apparatus (HCRA) and the DB-100 reflectometer were used to calculate independent values of emittance. Room temperature emittance determined by the two techniques, which are reported in Table 3, are in good agreement.

Table 3 also reports 2000°F emittance values calculated from the HCRA spectral data, and two

Table 4. Summary of results from EDAX, XRD, and EMP analysis of specimens

Spec. No.	Exposure/ # Cycles	Surface Analysis: EDAX COUNTS Cr	Co	Ni	XRD PHASES Cr_2O_3	$CoCR_2O_4$	NiO	EMP-WT % Cr	Ni	Co	O	OET+	EMP Line Scans: Oxide Thick μm	Alloy Depletion μm
I-227	AR	--	--	--	VS			56	6	2	32	4	5	19
I-230	AR	80	1	4										
I-229	R/6													
I-220	R/10	22	9	38									5	27
I-211	R/10				S	W	S						7	37
I-223	R/10				S	W	S							
I-224	R/10	35	7	28				25	32	7	32	4		
		10*	6*	49*										
		58**	4**	11**										
I-216	RL/6													
I-213	RL/10	30	13	28	S	W	S	24	27	11	34	4	5	31
													6	34
I-204	RA/5													
I-214	RA/5	27	6	19	S	VW	M						6	30
		5*	8*	41*										
I-212	RO/10	22	10	35	S	W	S						7	47

* Spot analysis of spherical oxide particle
** Spot analysis of suboxide
\+ Other elements total

values of emittance measured at 2000°F using the NASA Langley Research Center high temperature emittance apparatus (HTEA). The HTEA results are 0.04 less than the calculated values. Reference 11 reported the 2000°F emittance of statically oxidized Inconel 617 to be 0.84. These favorable comparisons support the use of room temperature spectral reflectance data to estimate the elevated temperature emittance of Inconel 617.

The effect of exposure conditions on normal spectral emittance of Inconel 617 is shown in Fig. 5. Spectral emittance data for specimens from all three exposure conditions are about 0.8 and higher over the wavelength range from 2 to 12 μm. The spectral emittance data for the statically oxidized specimen has a strong dip in the wavelength range from 12 to 25 μm. The differences in emittance of the statically oxidized specimen and the specimens exposed to reentry conditions result from the changes that occur in the surface oxide with reentry exposure.

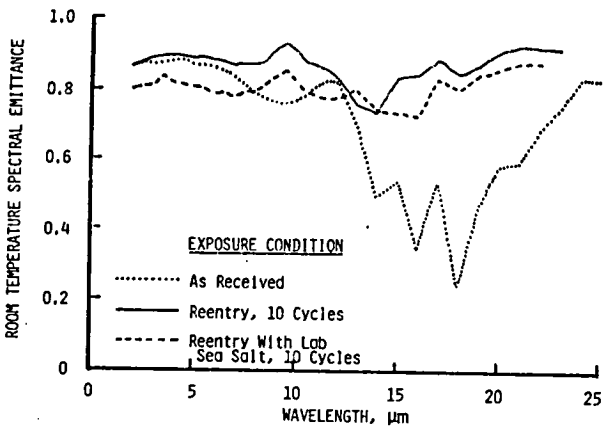

Fig. 5 Spectral emittance of Inconel 617 at room temperature.

Fig. 6 shows the spectral emittance of Cr_2O_3 and NiO which are the primary oxides of Inconel 617. The emittance of Cr_2O_3 is very much like the emittance of the statically oxidized specimen (Fig. 5). The spectral emittance of NiO has a peak in the wavelength range from 12 to 20 μm. As the fraction of NiO in the surface oxide increases with exposure to reentry conditions, the emittance of the surface assumes more of the characteristics of NiO and Cr_2O_3 shown by the data in Fig. 5.

Since the radiative heat shield functions at elevated temperature, its radiative properties at temperatures of the order experienced during reentry are of primary interest. Fig. 7 shows the calculated total normal emittance for 2000°F versus exposure cycles for different conditions. The emittance is greater than 0.8 for all exposure conditions and times. The emittance of specimens whose oxides were removed, including the specimen which had its oxide removed at the completion of all reentry exposure cycles, is greater than 0.8.

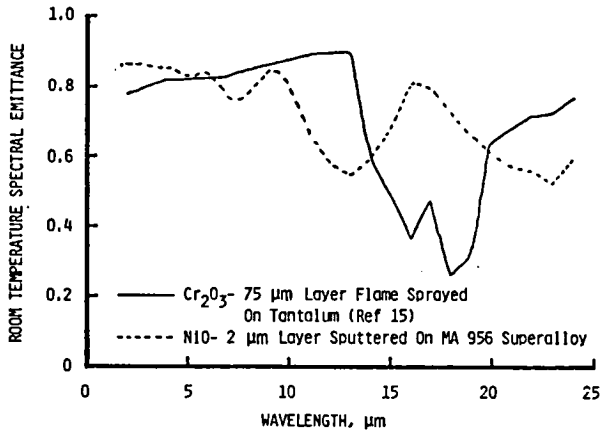

Fig. 6 Spectral emittance of oxides of Inconel 617 at room temperature.

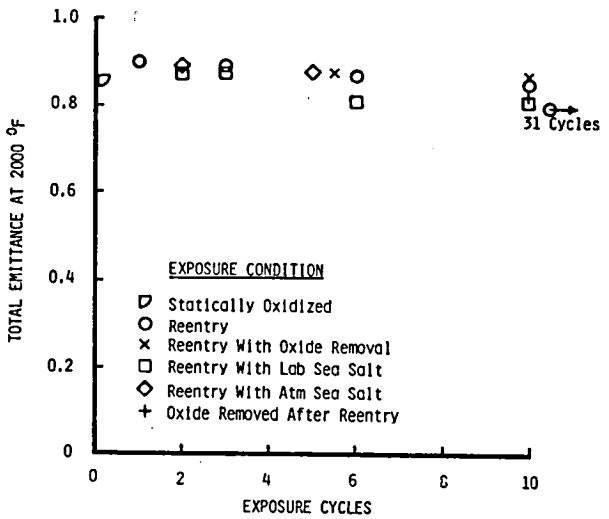

Fig. 7 Emittance of Inconel 617 at 2000°F.

Concluding Remarks

The response of Inconel 617 to simulated reentry with and without exposures to a seashore environment or a laboratory sea salt environment was studied and the following results were obtained.

1. There was no observable interaction between sea salt and the surface oxides of Inconel 617. The response of specimens subjected to reentry simulation testing with sea salt exposure was not significantly different from specimens exposed to reentry simulation alone. Any sea salt deposits at the oxide surface are very quickly volatilized during reentry testing leaving no residue.

2. The elevated temperature emittance of Inconel 617 was greater than 0.8 for all exposure conditions and times.

3. The mass loss of Inconel 617 exposed to simulated reentry is about 60% of the mass loss for the most severe case where the oxide is physically removed after each cycle of reentry exposure. The mass loss of specimens exposed to the combined reentry/sea salt environments is bounded by these data.

4. The substrate thickness change of Inconel 617 based on mass loss data is about 2-10 μm for 10 simulated reentry cycles.

5. The oxide layer of statically oxidized Inconel 617 is about 5μm thick and consists primarily of Cr_2O_3. The oxide thickness of Inconel 617 exposed to simulated reentry with or without sea salt is about 6 μm and consists of NiO and Cr_2O_3 with traces of $CoCr_2O_4$.

6. Selected diffusion of metal atoms from the alloy substrate to the oxide-metal interface results in an alloy depleted zone which ranges from 19 μm in thickness for a statically oxidized specimen to 47 μm for a specimen exposed to 10 cycles of simulated reentry with the oxide removed between reentry cycles. The thickness of the alloy depleted zone of specimens exposed to 10 cycles of simulated reentry with or without sea salt exposure is 30-35 μm.

References

1. Jackson, L. Robert; and Dixon, Sidney C.: A Design Assessment of Multiwall, Metallic Stand-Off, and RSI Reusable Thermal Protection Systems Including Space Shuttle Applications. NASA TM 8170, April 1980.

2. Taylor, Allan H.; and Jackson, L. Robert: Thermostructural Analyses of Structural Concepts for Hypersonic Cruise Vehicles. AIAA Paper No. 80-0407, Pasadena, CA, January 1980.

3. Devikis, W. D.; Miserentino, R.; Weinstein, I.; and Shideler, J. L.: Aerothermal Performance and Structural Integrity of a Rene' 41 Thermal Protection System in a Mach 6.6 Stream. NASA TN D-7943, 1975.

4. Gilbreath, W. P.: Degradation of Space Shuttle TPS Metals in Dissociated Oxygen. AIAA Paper No.72-262, San Antonio, TX, April 1972.

5. Tenney, D. R.; Young, C. T.; and Herring, H. W.: Oxidation Behavior of TD-NiCr in a Dynamic High Temperature Environment. Metallurgical Trans., Vol. 5, May 1974.

6. Schaffer, John W.; et al: Analytical and Experimental Evaluation of Flowing Air Test Conditions for Selected Metallics in a Shuttle TPS Application. NASA CR 2531, August 1975.

7. Young, C. T.; Tenney, D. R.; and Herring, H. W.: Dynamic Oxidation Behavior of TD-NiCr Alloy with Different Surface Pretreatments. Metallurgical Trans. A, Vol. 6A, December 1975.

8. Clark, Ronald K.; Webb, Granville L.; and dries, Gregory A.: Mechanical/Radiative Performance of Rene'41 in TPS Applications. Proceedings of NASA Symposium on Recent Advances in TPS and Structures for Future Space Transportation Systems, Dec. 13-15, 1983. NASA CP 2315, 1984.

9. Norris, Brian: High Temperature [1366K (2000°F)] Sheet Material Selection for Use for Thermal Protection Systems. ROHR Industries Inc. Report No. RHR 80-017, April 1980.

10. Cunnington, G. R.; Fretter, E. F.; and Clark, R. K.: Radiative Properties of a Nickel Based Superalloy - Inconel 617 - After Simulated Earth Reentry. AIAA Paper No. 82-0898, St. Louis, MO, June 1982.

11. Cunnington, G. R.; Funai, A. I.; and McNab, T.K.: Radiative Properties of Advanced Spacecraft Heat Shield Materials. NASA CR-3740, Nov. 1983.

12. Santoro, Gilbert J.: Hot Corrosion of Four Superalloys: HA-188, S-57, In-617, and TD-NiCrAl. Oxidation of Metals, Vol. 13, No. 5, 1979.

13. Foster, T.: Modification to the NASA LaRC/Aerotherm 100-kw Arc-Heated Wind Tunnel System. NASA CR-77262, Sept. 1977.

14. Edwards, S. Franklin; Kantsios, Andromicos G.; Voros, John P.; and Stewart, W. F.: Apparatus Description and Data Analysis of a Radiometric Technique for Measurement of Spectral and Total Normal Emittance. NASA TN D-7798, 1975.

15. Hosier, J. C.; and Tillack, D. J.: Inconel Alloy 617 - A New High Temperature Alloy. Metals Engineering Quarterly, Aug. 1972.

16. Clark, Ronald K.; Dicus, Dennis L.; and Lisagor, W. Barry: Emittance of TD-NiCr After Simulated Reentry Heating. Proceedings of the Fifteenth International Conference on Thermal Conductivity, held in Ottawa, Ontario, Canada, Aug 24-26, 1977. Thermal Conductivity 15 Edited by Vladimir V. Mirkovich, 1978.

1. Report No.	2. Government Accession No.	3. Recipient's Catalog No.
NASA TM-86293		

4. Title and Subtitle	5. Report Date
Response of Inconel 617 Superalloy to Combined Ground-Based and STS Reentry Exposure	August 1984
	6. Performing Organization Code: 506-53-33-01

7. Author(s)	8. Performing Organization Report No.
Ronald K. Clark Jalaiah Unnam	

9. Performing Organization Name and Address	10. Work Unit No.
NASA Langley Research Center Hampton, VA 23665	11. Contract or Grant No.

12. Sponsoring Agency Name and Address	13. Type of Report and Period Covered
National Aeronautics and Space Administration Washington, DC 20546	Technical Memorandum
	14. Sponsoring Agency Code

15. Supplementary Notes R. K. Clark, NASA Langley Research Center, Hampton, VA; J. Unnam, Analytical Service and Materials, Inc., Tabb, VA
This paper, available as AIAA Paper No. AIAA-84-1768, was presented at the 19th Thermophysics Conference in Snowmass, CO, June 25-28, 1984

16. Abstract

Inconel 617 is a nickel-based superalloy which is being considered for heat-shield applications because of its high-temperature strength, good oxidation resistance and high emittance of oxidized surfaces. While the effects of simulated reentry conditions on emittance and oxidation of Inconel 617 have been studied, the combined effects of the ground-based environment with sea salt exposure and the reentry environment have not been evaluated. Experimental results are presented to show the effects of environmental simulation including ground-based and reentry exposure on the emittance and oxidation of Inconel 617. Specimens were exposed to simulated reentry at a surface temperature of 2000°F in the Langley Research Center Hypersonic Materials Environmental Test System (HYMETS) Facility with and without alternate exposures to an atmospheric seashore environment or a laboratory sea salt environment. This paper presents emittance, mass loss, oxide chemistry, and alloy composition data for the specimens.

17. Key Words (Suggested by Author(s))	18. Distribution Statement
Environmental Effects Emittance Metallic Heat Shield Inconel 617 Superalloys	Unclassified-Unlimited Subject Category 26

19. Security Classif. (of this report)	20. Security Classif. (of this page)	21. No. of Pages	22. Price*
Unclassified	Unclassified	8	A02

* For sale by the National Technical Information Service, Springfield, Virginia 22161